

FINAL TECHNICAL REPORT

Award number: G12AP20113

Title: Fault slip and strain rates near western US population centers from inversion of geologic, seismologic and geodetic data

Period of award: 7/15/12 – 7/14/13

Principal Investigator:

Robert McCaffrey
Portland State University
Dept. of Geology
Portland OR 97207-0751
r.mccaffrey@pdx.edu

Abstract

This grant supported the PI's involvement in developing a geodetic model for the National Seismic Hazard Map of 2014. The results of that work are presented here in the form of Appendix A of Petersen et al. (2014)

Appendix A: NSHMP Block Model of Western US Active Tectonics

By R. McCaffrey¹, P. Bird², J. Bormann³, K. M. Haller⁴, W. H. Hammond³, W. Thatcher⁵, R. E. Wells⁵, Y. Zeng⁴

¹ Dept. of Geology, Portland State University, Portland OR

² Dept. of Earth and Space Sciences, University of California, Los Angeles, CA

³ Nevada Geodetic Laboratory, University of Nevada Reno, NV

⁴ USGS Golden, CO

⁵ USGS Menlo Park, CA

Abstract. We developed a block model of active faults in the western United States (WUS) in support of the 2014 National Seismic Hazards Mapping Project (NSHMP14).

The block model used source faults of NSHMP14 as block boundaries as much as reasonably possible with the aim of estimating slip rates on those faults. GPS-derived horizontal velocity data were compiled from seven regional solutions and rotated into a common North American reference frame. The GPS velocities were edited to remove outliers and a correction was made to account for elastic strain rates caused by locking on the Cascadia subduction zone. The GPS velocity field was used by the researchers to

assess and if necessary modify fault slip rates used in NSHMP14. Block models resulted in generally faster fault slip rates than adopted for NSHMP14.

Introduction

Block models of crustal deformation allow analysis and simultaneous interpretation of multiple types of data that relate to motions of the crust and slip rates on faults. The models are based on plate tectonic formulations, largely that crustal blocks, like tectonic plates, rotate about Euler poles. In addition, the block models can account for elastic strain rates that occur near faults due to friction on them and distributed strain rates that result from slip on multiple, closely-spaced faults. Elastic strain rate corrections are needed to interpret decade-scale GPS velocity data in terms of longer-term fault motions. This chapter reports on the development of the WUS block model WUS5 used to interpret GPS velocity data in the context of fault slip rates used in NSHMP14.

Block model WUS5

We developed a block model, called WUS5, that includes 70 blocks in the WUS (fig. A-1). To maintain continuity with UCERF-3, this model also includes the blocks in California used in the UCERF-3 average block model (ABM) but the number of fault segments was decreased for simplicity. In WUS5, the block boundaries outside California were greatly modified from those used in UCERF-3.

[Figure A-1]

The initial block model was adapted from those of McCaffrey (2005) and Meade and Hager (2005) for California, McCaffrey and others (2007) for the Pacific Northwest, Payne and others (2008; 2012) for the Wasatch and Snake River Plain region, Hammond and others (2011) for the Walker Lane area, and Kreemer and others (2010) for the southern Great Basin. The initial model was modified to connect the separate regions and to follow more closely the set of NSHMP14 target faults (fig. A-2). The block boundaries include most NSHMP14 faults with slip rates of greater than 1 mm/yr. Other modifications were to break up the original long thin blocks, whose motions are difficult to resolve, into smaller entities. Block boundaries were used to separate regions of differing strain rates even though we did not always believe the boundaries themselves

are areas of significant slip; in this case some models included estimates of the off-fault strain rates, which are not considered in NSHMP14.

[Figure A-2.]

In many regions the GPS data cannot distinguish between slip on multiple, closely-spaced individual faults and more uniformly distributed strain rates. For example, as Payne and others (2012) show, the CTBt block, north of the Snake River Plain, could be subdivided along known faults (Lemhi, Beaverhead, Lost River, etc.) but in doing so the fit to the GPS data does not change. Hence the GPS velocities do not provide additional information on the slip rates of these faults. There are many similar examples throughout the western US, most notably Nevada Basin and Range where we assigned block boundaries based on perceived spatial changes in strain rates, but without expectation to constrain slip rates on them.

GPS Data

GPS velocities were compiled from seven velocity fields, listed in table A-1 and shown in figure A-3a. Some of the velocity fields encompassed the entire boundary while others were more regional in scale.

Table A-1. Velocity fields used and rotation into North America reference frame.

Field	GPS	Long.	Lat.	Omega	Reference
PNW	696	282.1	24.9	0.022	McCaffrey and others (2013)
CMM4	551	285.3	35.3	0.020	Shen and others (2011)
PBO	942	331.0	-40.0	0.014	PBO 2011.08.01
UNR	219	273.9	-2.9	0.184	Hammond and others (2011)
PANGA	308	299.6	43.0	0.023	PANGA 2012.03.05
SOPAC	1252	273.5	-4.9	0.185	SOPAC 2012.07.06
SHEN	1997	69.1	-18.4	0.011	Z-K Shen, unpublished

GPS is the number of velocities in the solution. Long., Lat., and Omega give the Euler pole used to rotate the velocity field into the North American reference frame.

[Figure A-3.]

In addition to the GPS velocities, for which we used only the horizontal components in the block modeling, vertical velocities derived from leveling surveys (Burgette and

others, 2009) were used to help constrain the locking on the Cascadia subduction fault; see McCaffrey and others (2013) for details. The vertical rates were not distributed with the corrected horizontal velocities or used in subsequent modeling.

Reference Frame

Using the block model WUS5 and the program *tdefnode* (McCaffrey, 2002; 2009), the velocity fields were rotated into a common reference frame defined by the North American (NoAm) block. This is accomplished by rotating each velocity field to minimize the velocities of the GPS sites on the reference (NoAm) block. For velocity fields with that have no or few sites on NoAm, the reference frame rotations result from aligning it with the other velocity fields. To get the rotation of a velocity field (V) relative to NoAm (N) we solve:

$$v\Omega_N = v\Omega_B + {}_B\Omega_N \quad (1)$$

where B represents a block. Since ${}_B\Omega_N$ is the same for all velocity fields, $v\Omega_B$ is estimated by minimizing the velocity residuals for velocity field V in the block B . And since $v\Omega_N$ is the same for all blocks, it is estimated by minimizing velocity residuals in all the blocks. In the inversion, only $v\Omega_N$ and ${}_B\Omega_N$ are estimated. Using this approach, the velocity fields do not require common sites and not all need sites on the reference block. Each velocity field, however, must cover multiple blocks.

Most of the velocity fields used were already close to being in the North American reference frame and needed only small adjustments, on the order of 1 mm/yr or less to align with the average field. Two fields (UNR and SOPAC) were initially in a global (IRTF) reference frame and required adjustments of closer to 15 mm/yr (the adjustments are by rotations so will vary across the network).

Data editing

After initial runs of the block model, during which the velocity fields were rotated into a common reference frame, the velocities were edited by visual inspection and by examining the statistics and misfits. For mature velocity fields, in the absence of co-seismic signals, the velocities vary spatially in a very smooth manner. Hence, if a single velocity was very different from nearby velocities in either azimuth or magnitude or both, we removed it from the data set. In other cases, the deviation of a velocity was not

visually obvious but was statistically different from nearby velocities, and it was removed.

We also excluded velocities with high uncertainties since they add little information in a least-squares inversion. The uncertainty cutoffs applied were 0.8 mm/yr for PNW and UNR fields and 1.0 mm/yr for the others. In addition we applied a ‘floor’ to the uncertainties in the sense that any formal uncertainty of less than 0.3 mm/yr was set to 0.3 mm/yr. This limitation was aimed to avoid sites with very low uncertainties, some less than 0.1 mm/yr, from dominating the least-squares solution. It also represents some expected level of uncertainty among the reference frames. We removed ‘equated’ sites from some of the solutions; these are nearby sites whose data were combined in the GAMIT/GLOBK velocity analysis to estimate a single velocity and uncertainty. Sites within about 30 km of five actively-deforming volcanic regions were also removed (Mt. St. Helens, Mono Lake, Rainier, Shasta and Sisters).

Cascadia elastic strain rate correction

Locking on the Cascadia subduction zone was estimated by inverting the horizontal GPS and vertical leveling data (fig. A-4). The details of the procedure are outlined in McCaffrey and others (2013) but in this application we used all seven velocity fields. The geometry of the Cascadia plate interface was taken from McCrory and others (2003). The elastic velocities due to fault locking were calculated using dislocations in an elastic half-space following Okada (1985) and using the Savage (1983) backslip approach; the backslip component is $-\varphi \mathbf{V}$ where φ is a locking fraction and \mathbf{V} is the relative motion vector across the fault. The vector \mathbf{V} is derived from the blocks’ Euler poles and φ is estimated in the inversion. For this calculation we parameterized the distribution of the locking fraction φ with a defined function describing the change in locking with depth along profiles down the dip of the slab interface. The parameterization follows Wang and others (2003); $\varphi = 1.0$ at depths shallower than the top, z_u , of what they call the effective transition zone (ETZ) and $\varphi = 0.0$ at depths below the bottom, z_l , of the ETZ. Within the ETZ

$$\varphi(z) = [\exp(-z'/\gamma) - \exp(-1/\gamma)]/[1 - \exp(-1/\gamma)] \quad (2)$$

where $z' = (z - z_u) / (z_l - z_u)$ and γ is a shape factor. McCaffrey and others (2007) modified Wang’s representation to allow for a more general case. Equation (2), in

addition to constraining φ to decrease with depth, forces the slope $d\varphi/dz$ to increase or remain approximately constant with depth (see Wang and others 2003; their figure 8). To allow the slope to decrease with depth, we use a new parameter, γ' , and make the substitution in (2) of $\gamma = \gamma'$ when $\gamma' \leq 5$, and $\gamma = \gamma' - 10$ when $5 < \gamma' \leq 10$. For values of γ' between 0 and 5, $\varphi(z)$ is given by (2) and for γ' between 5 and 10, $\varphi(z)$ is (2) reflected about the φ and z axes (McCaffrey and others, 2007; their figure 7a).

[Figure A-4.]

The Cascadia slab interface was divided into 34 profiles starting at the deformation front, running perpendicular to it and in the down-dip direction. The profiles were then discretized by node positions in longitude, latitude and depth and the value of φ was estimated at each node (depth) following the function (2). In the inversion, the parameters γ' , z_l and z_u were estimated for each profile, subject to along-strike smoothing. Smoothing is applied by using a penalty function to damp the Laplacian of the φ distribution (McCaffrey and others, 2013). The ‘best-fit’ set of parameters was found by minimizing the sum of the data misfit (reduced chi-square) plus the penalty function.

The model used to estimate Cascadia locking included all the blocks (fig. A-1) while solving for their angular velocities but not internal strain within them. The motion of the Juan de Fuca plate (JdFa) was estimated in the inversion using spreading rates at the Juan de Fuca Ridge (DeMets and others, 2010) and fixing the Pacific – North America pole. The motion of JdFa relative to the fore-arc blocks give the slip vector \mathbf{V} used in the calculation of elastic strain at the Cascadia subduction zone. Once a best-fit set of parameters was determined, they were used to solve the forward problem to estimate a velocity at each GPS site arising from Cascadia locking (fig. A-4). These velocities were then subtracted from the observed site velocities and 10 percent of the locking velocities was added to the velocity uncertainties as follows:

$$\sigma_{\text{new}} = \sqrt{[\sigma_{\text{old}}^2 + (0.10 * V_{\text{lock}})^2]} \quad (3).$$

The resulting corrected velocity field is shown in figure A-3b.

Geologic Slip Rates

In block models, geologic data, that is, estimated or observed slip rates on faults by geologic means, can be used to constrain the motions of blocks in a formal inversion,

since the fault slip rate is simply the relative motions of the blocks across the boundary. The WUS5 block model does not provide a one-to-one correspondence between NSHMP14 geologic slip rate estimates and block boundaries (fig. A-2), largely for the reason noted above, that the block models cannot provide unique information on closely-spaced faults and therefore not every fault is on a block boundary. Even using strain rates within the blocks does not permit a unique slip rate estimate on the interior faults. Models that report slip rates on closely spaced faults are basing those rates on geologic data, not on GPS.

The source of consensus geologic rates was the 2008 slip rate database with a few updates (Haller and Wheeler, 2008a, 2008b). For the block models, that include only horizontal long-term motions, the fault-parallel slip rates were converted to horizontal (heave) rates assuming the dip angles given in the database. For comparison with the other model results, the model predicted horizontal rates V_h were converted back to along-dip slip rates V_{ds} using the same dip angles; $V_{ds} = V_h / \cosine(\text{dip})$. Unfortunately, most of the fault slip rates were estimated from throw observations with little knowledge of dip angles, so the horizontal rates used in the block modeling are poorly constrained. Also available to the modeling were fault slip rates calculated by P. Bird (Appendix C), using the technique described by Bird (2007), and rates taken from the literature and listed in McCaffrey and others (2007).

Block model results with *tdefnode*

The WUS5 block model was run using the inversion program *tdefnode*, which is a modification of *defnode* (McCaffrey, 2002, 2009). Two runs were done, one of the entire WUS5 model and another that excluded California (WUS5-noCA; table A-2). As noted above, the representation of the UCERF-3 block model in California was coarsened, so the fit to the data was degraded. The reduced chi-square χ_η^2 misfit is large for these models compared with models of the US Pacific Northwest using a single velocity field that typically have χ_η^2 less than ~ 2 (McCaffrey and others, 2013). We attribute this to the use of multiple velocity fields that estimate velocities and uncertainties in different ways and to a heterogeneous set of observed fault slip rates.

Table A-2. Model run statistics.

Model	GPS/Nrms	SR/Nrms	#Parameters	χ^2_{η}
WUS5	12385/3.1	1028/4.2	564	10.4
WUS5-noCA	6821/2.1	424/4.2	353	5.2

GPS and SR give the number of GPS and slip rate observations, respectively. Nrms is the normalized rms of the misfit to the data type. The reduced chi-square is χ^2_{η} .

Slip rates derived from block model

The block model was used by two groups to estimate fault slip rates; McCaffrey (RM) used *tdefnode* (McCaffrey 2002; 2009) and Hammond and Bormann (2013; HB) used the method described in Hammond and others (2011, see also Appendix B). The block models made estimates for 114 of the 294 faults in the USGS database, including most of those with published slip rates exceeding 1 mm/yr. The two inversions used the same block geometry and fault dips and generally the same formulation, but differed in details of the implementation and the data (Appendix 2). A major difference was the level of off-fault strain rates allowed within the block. The RM model allowed more strain within blocks than did HB resulting in faster fault slip rates in the HB model (fig. A-5A). Both block inversions resulted in generally faster slip rates than in the USGS database (figs. A-5B and A-5C). This latter result suggests that the GPS velocity fields may be indicating more total moment in the faults than is implied by the USGS database. This result is consistent with the Zeng and Shen fault-based inversion (Appendix D) who forced a fit to the geologic slip rates and estimated much higher off-fault moment rates than the models that did not (Appendix E) - a full ten times more than the HB model. Hence, there is information in the geodetic data that is not incorporated into NSHMP14, which should be among the targets of research prior to the next NSHMP.

[Figure A-5.]

Internal block strain rates

Along with the rotational components of the blocks, uniform strain rates are estimated for them (fig. A-6).

The horizontal strain rate tensor for a spherical Earth is given by Savage and others (2001) - the east and north velocities are:

$$\begin{aligned} V_{\lambda}(\lambda, \theta) &= e_{\text{ss}} R_e \sin \theta_0 (\lambda - \lambda_0) + e_{\text{se}} R_e (\theta - \theta_0) \\ V_{\theta}(\lambda, \theta) &= e_{\text{ss}} R_e \sin \theta_0 (\lambda - \lambda_0) + e_{\text{ee}} R_e (\theta - \theta_0) \end{aligned} \quad (4)$$

where λ is longitude, θ is co-latitude, R_e is the radius of the Earth, e_{ij} is the strain rate tensor, and (λ_0, θ_0) is the centroid of the block. When applied, the three independent components of the symmetric strain rate tensor, e_{ss} , e_{se} , and e_{ee} , are formally estimated in the inversion (McCaffrey, 2005). These terms are intended to represent deformation due to un-modeled faults within the blocks. In the WUS outside California, the internal strain rates are generally low, less than 10 nanostrain/year (1 nanostrain/year = 10^{-9} year $^{-1}$). The fastest straining regions are the Yakima fold-thrust belt in Washington and parts of the Basin and Range (fig. A-6).

[Figure A-6.]

Summary

A working group developed a block model for the WUS to incorporate GPS data into the assessment of slip rates to be adopted by NSHMP14. The model was run through two separate codes and predicted slip rates for a subset of the 2014 source faults. The block models showed considerable scatter in their agreement on slip rates but both were consistently faster than the adopted consensus geologic rates. The WUS outside California poses a particular difficulty for geodetic methods to contribute to hazards assessment due to the low density of GPS stations and low slip rates on faults. Continued densification of the geodetic networks and longer observation spans, to reduce errors, will enhance the utility of GPS for earthquake hazards assessment.

References

- Bird, P., (2007). Uncertainties in long-term geologic offset rates of faults: General principles illustrated with data from California and other western states, *Geosphere*, 3, 577-595, doi: 10.1130/GES00127.1.
- Burgette, R.J., R.J. Weldon, and D.A. Schmidt, (2009). Interseismic uplift rates for western Oregon and along-strike variation in locking on the Cascadia subduction zone: *J. Geophys. Res.*, 114, B01408, doi:10.1029/2008JB005679.
- DeMets, C., R. G. Gordon and D. F. Argus, (2010). Geologically current plate motions, *Geophys. J. Int.*, doi: 10.1111/j.1365-246X.2009.04491.x

- Haller, K.M., and Wheeler, R.L., 2008a, Parameter for faults in the Intermountain West, *in* Peterson, M.D., and others, Documentation for the 2008 update of the National Seismic Hazard Maps: U.S. Geological Survey Open-File Report 2008-1128, p. G-1–18.
- Haller, K.M., and Wheeler, R.L., 2008b, Parameter for faults in the Pacific Northwest, *in* Peterson, M.D., and others, Documentation for the 2008 update of the National Seismic Hazard Maps: U.S. Geological Survey Open-File Report 2008-1128, p. H-1–6.
- Hammond, W. C., Blewitt, G., and Kreemer, C., (2011). Block modeling of crustal deformation of the northern Walker Lane and Basin and Range from GPS velocities: *J. Geophys. Res.*, 116, B04402, doi:10.1029/2010JB007817.
- Hammond, W. C., and J. Bormann (2013). Appendix B. A Block Model of Western US Tectonic Deformation for the 2014 National Seismic Hazard Maps from GPS and Geologic Data, this report.
- Kreemer, C., Blewitt, G., and Hammond, W. C., (2010). Evidence for an active shear zone in southern Nevada linking the Wasatch fault to the Eastern California shear zone, *Geology*, 38, 475–478, doi: 10.1130/G30477.1.
- McCaffrey, R., (2002). Crustal block rotations and plate coupling, *in* Plate Boundary Zones, S. Stein and J. Freymueller, editors, AGU Geodynamics Series 30, 101–122.
- McCaffrey, R., (2005). Block kinematics of the Pacific - North America plate boundary in the southwestern US from inversion of GPS, seismological, and geologic data, *J. Geophys Res.*, 110, B07401, doi:10.1029/2004JB003307.
- McCaffrey, R., (2009). Time-dependent inversion of three-component continuous GPS for steady and transient sources in northern Cascadia: *Geophys. Res. Lett.*, 36, L07304, doi:10.1029/2008GL036784.
- McCaffrey, R., A. I. Qamar, R. W. King, R. Wells, G. Khazaradze, C. A. Williams, C. W. Stevens, J. J. Vollick, and P. C. Zwick, (2007). Fault locking, Block Rotation and Crustal Deformation in the Pacific Northwest, *Geophys. J. Int.*, v. 169, p. 1315–1340, doi:10.1111/j.1365-246X.2007.03371.x.
- McCaffrey, R., R. W. King, S. J. Payne, and M. Lancaster, (2013). Active Tectonics of Northwestern US inferred from GPS-derived Surface Velocities, *J. Geophys. Res.*, 118, doi:10.1029/2012JB009473.
- McCrory, P. A., J. L. Blair, D. H. Oppenheimer and S. R. Walter (2003). Depth to the Juan de Fuca slab beneath the Cascadia subduction margin: A 3-D model for sorting earthquakes: U.S. Geological Survey Digital Data Series, 1 CD-ROM.
- Meade, B., and B. H. Hager (2005). Block models of crustal motion in southern California constrained by GPS measurements, *J. Geophys. Res.* 110, doi:10.1029/2004JB003209.
- Okada, Y. (1985). Surface deformation due to shear and tensile faults in a half-space, *Bull. Seismol. Soc. Amer.*, 75, 1135–1154.
- Payne, S. J., R. McCaffrey, and R.W. King (2008). Strain rates and contemporary deformation in the Snake River Plain and surrounding Basin and Range from GPS and seismicity, *Geology*, 36, 647–650.

- Payne, S. J., R. McCaffrey, R.W. King and S.A. Kattenhorn (2012). A new interpretation of deformation rates in the Snake River Plain and adjacent Basin and Range regions based on GPS measurements, *Geophys. J. Inter.*, 189, 101-122, doi: 10.1111/j.1365-246X.2012.05370.x.
- Savage, J. C. (1983). A dislocation model of strain accumulation and release at a subduction zone, *J. Geophys. Res.*, 88, 4984-4996.
- Savage, J. C., W. Gan, and J. L. Svarc (2001). Strain accumulation and rotation in the eastern California shear zone, *J. Geophys. Res.* 106, 21,995-22,007.
- Shen, Z-K., R. W. King, D. C. Agnew, M. Wang, T. A. Herring, D. Dong, and P. Fang (2011). A unified analysis of crustal motion in Southern California, 1970-2004: The SCEC crustal motion map, *J. Geophys. Res.*, 116, doi: 10.2019/2011JB008549.
- Wang, K., R. Wells, S. Mazzotti, R. D. Hyndman and T. Sagiya (2003). A revised dislocation model of interseismic deformation of the Cascadia subduction zone, *J. Geophys. Res.*, 108, 2026, doi:10.1029/2001JB00122.

Other Related Publications:

- Payne, S. J., R. McCaffrey, R.W. King, and S. A. Kattenhorn, A new interpretation of deformation rates in the Snake River Plain and adjacent basin and range regions based on GPS measurements, *Geophysical Journal International*, doi:10.1111/j.1365-246X.2012.05370.x, 2012.
- Pearson, C. F., R. S. Snay, R. McCaffrey, Towards an integrated model of the interseismic velocity field along the western margin of North America, *International Association of Geodesy Symposia*, in press, 2013.
- Petersen, M. D., Y. Zeng, K. M. Haller, R. McCaffrey, W. H. Hammond, P. Bird, M. Moschetti, and W. Thatcher, GPS and Geology Based Slip-Rate Models for the Western U.S. (Not Including California) National Seismic Hazard Maps, USGS OFR-???, in press, 2014.
- McCaffrey, R., R. W. King, S. J. Payne, and M. Lancaster, (2013). Active Tectonics of Northwestern US inferred from GPS-derived Surface Velocities, *J. Geophys. Res.*, 118, doi:10.1029/2012JB009473.
- Payne, S. J., R. McCaffrey, and S. A. Kattenhorn, Extension Driven Right-lateral Shear in the Centennial Shear Zone Adjacent to the Eastern Snake River Plain, Idaho, *Lithosphere*, doi: 10.1130/L200.1, 2013.
- Wells, R., and R. McCaffrey, Rotation of the Cascade Arc, *Geology*, 41, 1027-1030, doi: 10.1130/G34514.1 2013.

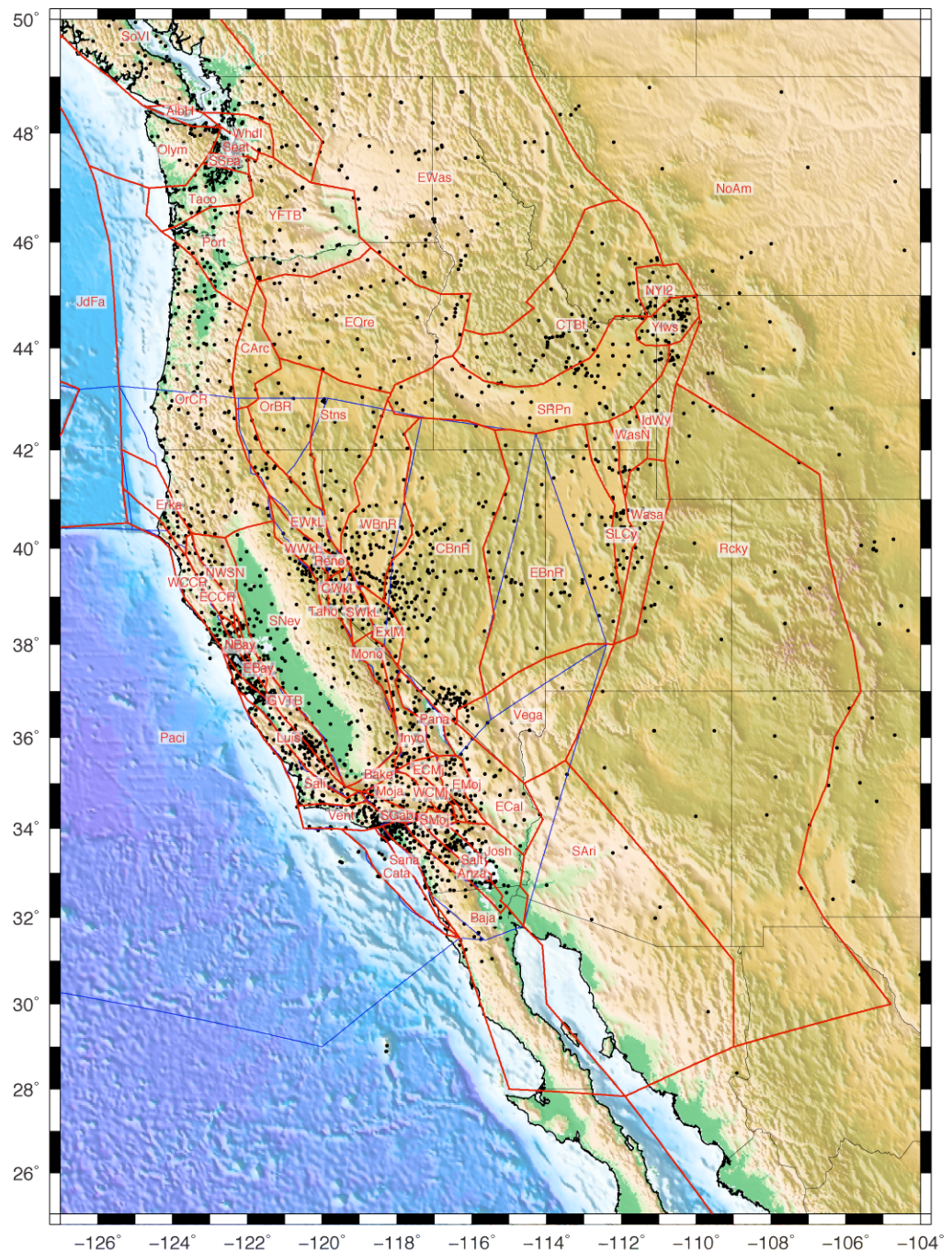


Figure 1. Map of western US showing block boundaries for WUS5 (red) and California's UCERF-3 ABM (blue). Black dots show locations of GPS velocities used. Four-letter codes are block names.

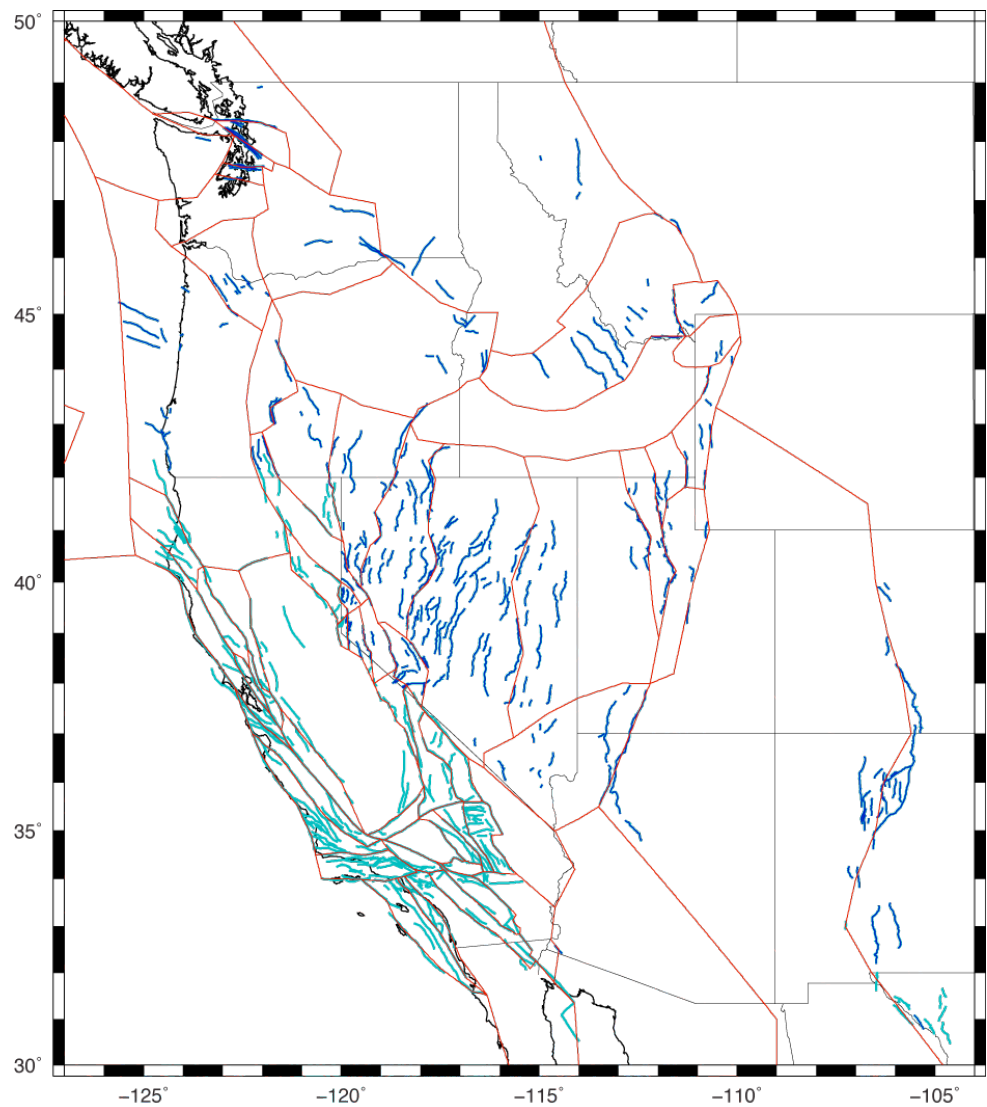


Figure 2. Block model boundaries (red lines) and NSHMP source faults. Turquoise are UCERF-3 faults and blue are ‘non-California’ faults.

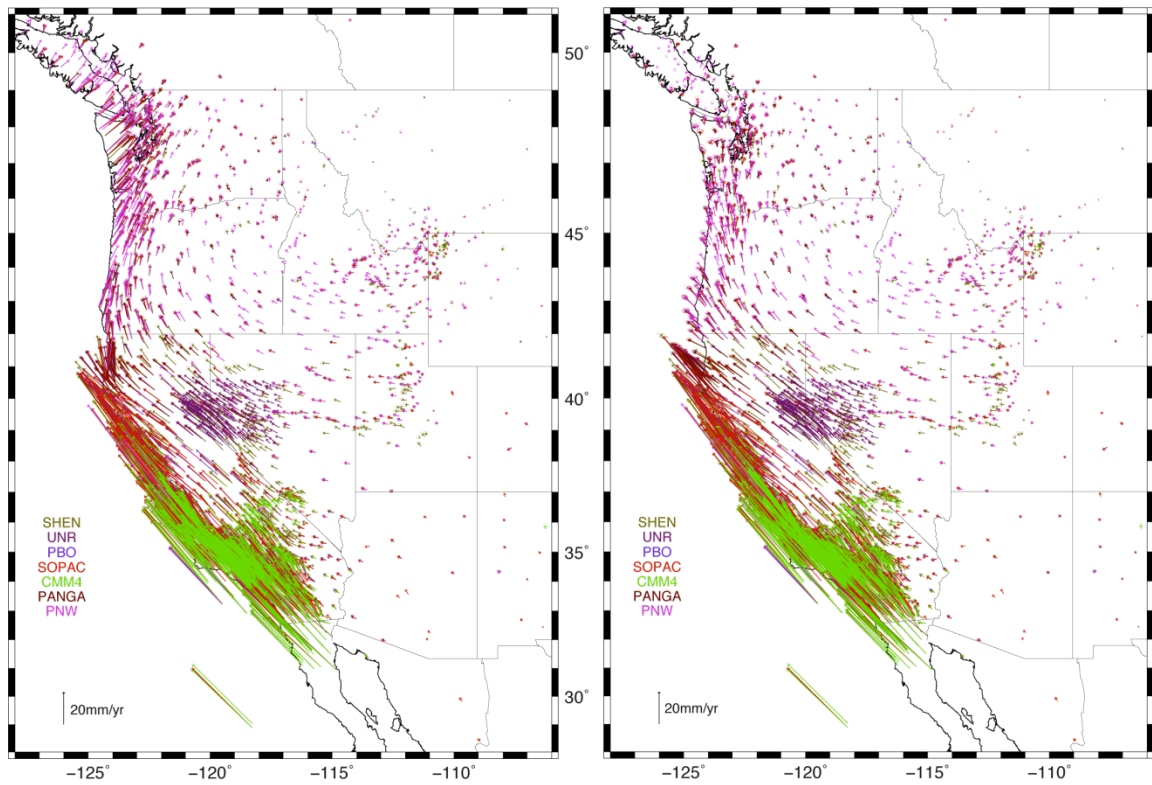


Figure 3. Original velocity fields (left) rotated into North America reference frame. Corrected velocity fields (right) with effects of Cascadia locking removed. Vector colors correspond to source.

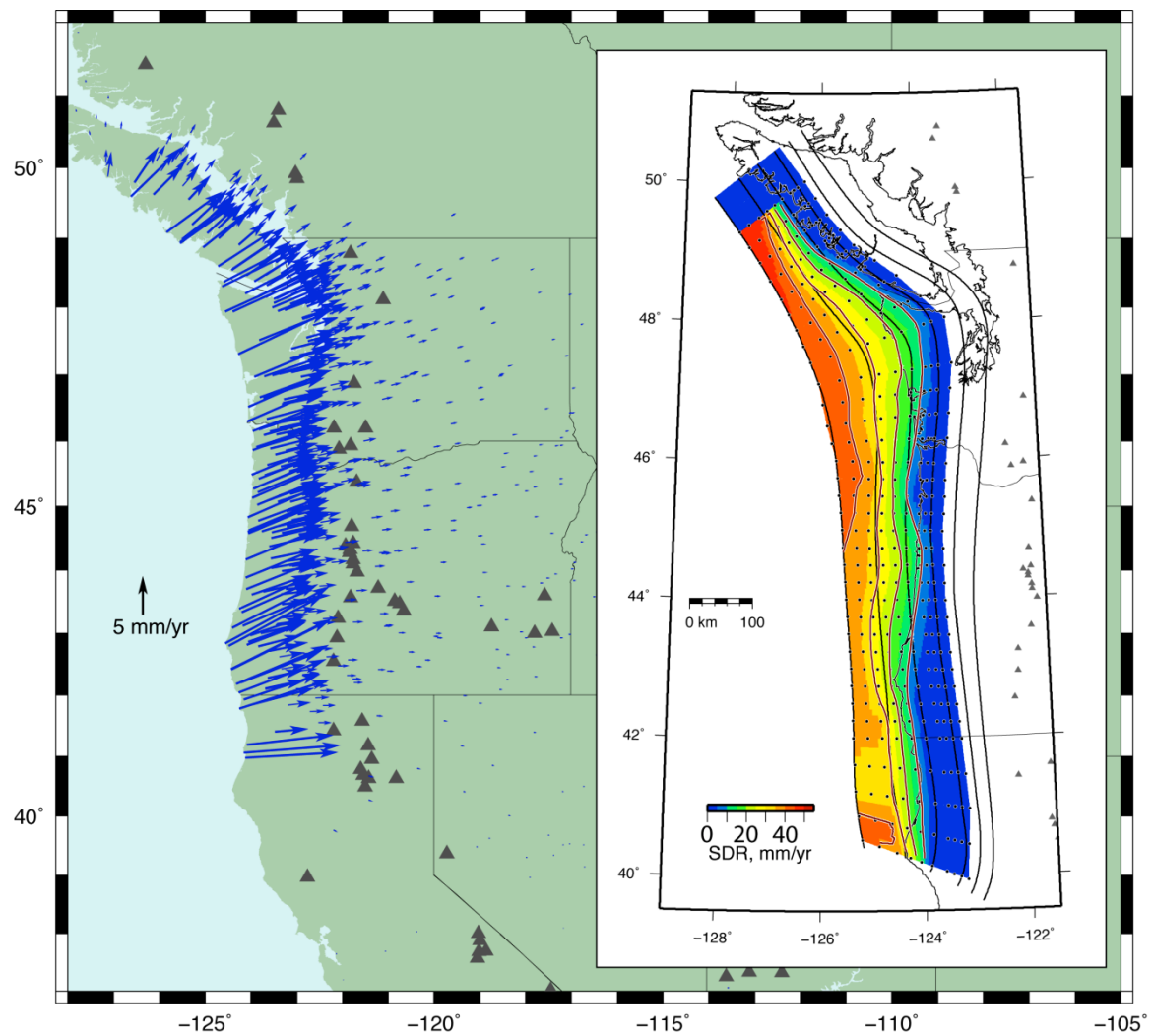


Figure 4. Corrections to velocity field for locking at the Cascadia subduction zone. Insert shows locking model; SDR is the slip deficit rate; dots are node positions; black lines are 10-km slab contours and red lines are 10 mm/yr SDR contours. Triangles are locations of volcanoes.

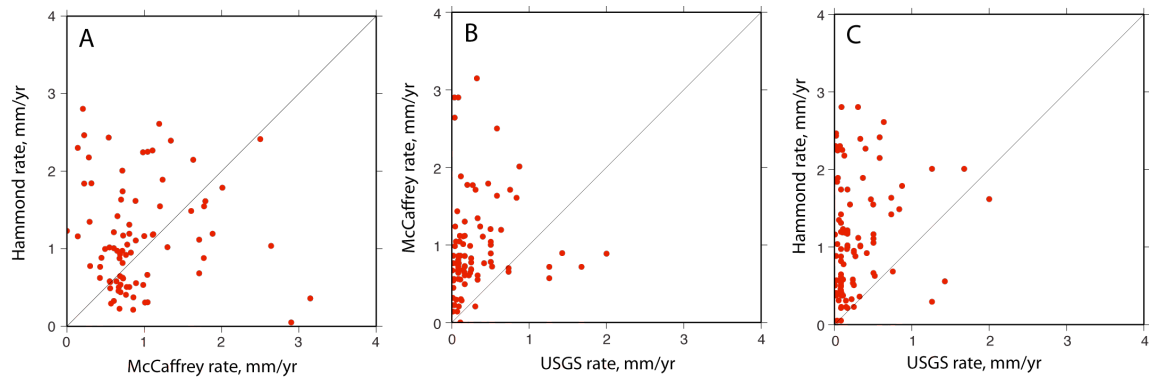


Figure 5. Comparison of fault slip rates (total rate) for the McCaffrey and Hammond/Bormann block models and the USGS adopted rates.

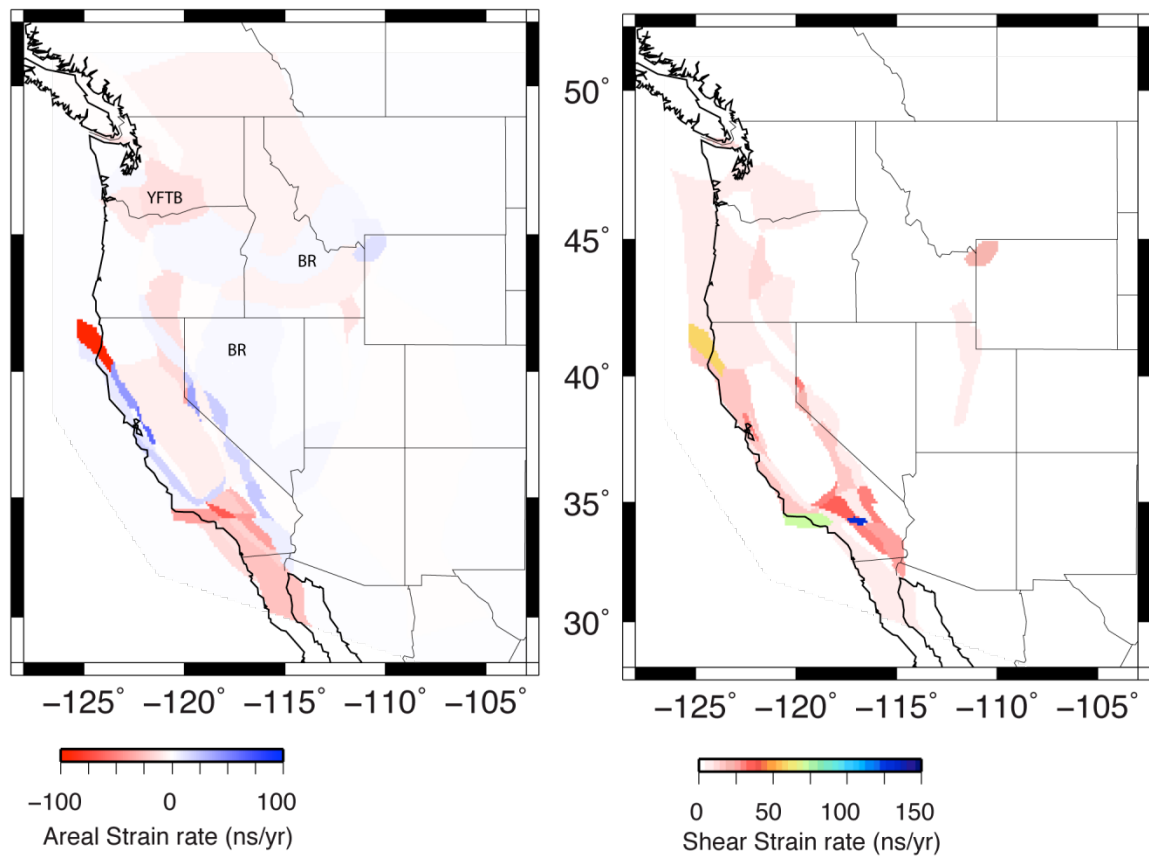


Figure 6. Strain rates within blocks estimated from GPS data and *tdefnode*. BR = Basin and Range; YFTB = Yakima fold-thrust belt. Negative strain rates are contraction; positive are extension.